arXiv:1605.06082v1 [cond-mat.stat-mech] 19 May 2016

An Apparent Dissociation Transition in Anharmonically Bound 1D Systems

D. J. Priour, Jr[1] and Christopher Watenpool[2]

[1]*Department of Physics & Astronomy, Youngstown State University, Youngstown, OH 44555, USA*
[2]*Department of Electrical Engineering, Youngstown State University, Youngstown, OH 44555, USA*

(Dated: May 20, 2016)

For diatomic molecules and chains bound anharmonically by interactions such as the Lennard Jones and Morse potentials, we obtain analytical expressions for thermodynamic observables including the mean bond length, thermally averaged internal energy, and the coefficient of thermal expansion. These results are valid across the shift from condensed to gas-like phases, a dissociation transition marked by a crossover with no singularities in thermodynamic variables for finite pressures, though singular behavior appears in the low pressure limit. In the regime where the thermal energy $k_{\rm B}T$ is much smaller than the dissociation energy D, the mean interatomic separation scales as $\langle l\rangle = R_e + \mathcal{B}(PR_e/k_{\rm B}T)^{-2}e^{-D/k_{\rm B}T}\,(D/k_{\rm B}T)^{1/2}$ for both the Morse and Lennard Jones potentials where p is a pressure term, R_e is the $T=0$ bond length, and $\mathcal{B}$ is a constant specific to the potential.

PACS numbers: 64.60.De,61.43.-j,34.80.Ht,51.30.+i

Potentials used to describe interactions among atoms such as the Lennard Jones potential [1] (e.g. Van der Waals couplings among noble gas atoms such as Argon) and the Morse potential [2] (for bonding with significant covalent character) contain attractive and repulsive terms. Whereas the attractive component decays at large distance, the repulsive piece decays even more rapidly in the large separation regime while rising sharply when atoms are in proximity where Pauli Exclusion effects play a role as atomic cores begin to overlap. With the combination of attractive and repulsive terms, there is a potential minimum at the equilibrium separation R_e with harmonic (parabolic) dependence in the vicinity of R_e and increasingly asymmetric and anharmonic character for significant deviations from R_e caused, e.g., by thermal fluctuations in the high temperature regime. Whether due to Van der Waals coupling as in the Lennard Jones model or the sharing of charge represented by the Morse potential, entropic effects drive dissociation despite the attractive component, except at $T=0$ where thermal fluctuations are absent. Nevertheless, confinement of the system volume for finite temperatures is realized by taking into consideration a pressure term (incorporated in the 1D context as a finite cost per length of elongating the system, such as a chain of identical atoms), which precludes indefinite expansion of the system.

In this work, we operate in terms of three distinct energy scales relevant to both the Morse and Lennard Jones potentials; the thermal energy $k_{\rm B}T$, the dissociation energy D needed to completely separate an interacting pair of atoms, and the pressure confinement scale pR_e. For high T, where $k_{\rm B}T \gg D$ the competition among pR_e and $k_{\rm B}T$ dominates, and the state is well approximated as an ideal gas. On the other hand, for low T, where $k_{\rm B}T \ll D$, there is a more subtle interplay among p, T, and D with a crossover with decreasing p from a condensed state ($\langle l\rangle \approx R_e$) to a diluted gas-like state ($\langle l\rangle \gg R_e$). For a more detailed description of dissociation, we obtain analytical expressions for thermodynamic variables of interest valid across the shift from the condensed to gas-like states in the low to intermediate temperature regimes. With a unified treatment applied to both the Lennard Jones and Morse cases, we find strong qualitative similarities in molecular dissociation phenomena despite distinct bonding physics driving the potentials.

With interactions only among nearest neighbors, the system energy is $E=\sum_i P_i^2/2M+\sum_i V(R_{i+1}-R_i)+pL$ with the sum over the N members of the chain, L being the total system size. Since atomic momenta and spatial coordinates are not coupled, apart from a contribution $Nk_{\rm B}T/2$ to the internal energy (and $Nk_{\rm B}/2$ to the specific heat), one need only consider site positions in sampling system configurations. We obtain thermodynamic variables of interest from the partition function Z; though in general the rapid scaling of configuration space with the number of system components precludes an analytical calculation of Z, we decouple the calculation of Z by describing the system in terms of the separation among adjacent sites $\Delta_i \equiv R_{i+1}-R_i$ instead of the absolute atomic coordinates R_i [3, 4]. Noting that $L = R_N - R_1 = \Delta_{N-1}+\Delta_{N-2}+\ldots+\Delta_1$, the partition function may be factorized as $Z=\hat{Z}^{N-1}$ where $\hat{Z}=\int_0^\infty \exp(-\beta[V(\Delta)+p\Delta])d\Delta$. In this manner, the calculation for a chain of arbitrary length is reduced to the case of a single atomic pair separated by a distance Δ (subsequently labeled as R), subject to an asymptotically linearly diverging effective potential $V(R)+pR$.

It is convenient to operate in terms of dimensionless energy variables $\varepsilon \equiv \beta D$ and $\eta \equiv pR_e$ as well as the ratio $\gamma \equiv pR_e/D = \eta/\varepsilon$ characterizing the strength of the pressure energy scale in relation to the dissociation energy. Salient thermodynamic variables may then be calculated by differentiating with respect to ε and η, such as $\langle E\rangle = -\partial/\partial\beta \ln Z = -(\varepsilon Z_\varepsilon + \eta Z_\eta)\beta^{-1}Z^{-1}$ for the internal energy where $Z_\varepsilon \equiv \partial Z/\partial\varepsilon$ and $Z_\eta \equiv \partial Z/\partial\eta$. Though having different functional forms, $V_{\rm LJ} = BR^{-12} - AR^{-6}$

(Lennard Jones) and $V_{\rm M} = -D + D\{-1 + \exp[-a(R - R_e)]\}^2$ (Morse), $V_{\rm LJ}$ and $V_{\rm M}$ are amenable to the same analysis with qualitatively similar results in both cases.

When expressed in terms of D and the reduced separation $r \equiv R/R_e$, $V_{\rm LJ}$ and $V_{\rm M}$ are both of the form $V(r) = -D + D[\chi(r) - 1]^2$ where $\chi_{\rm LJ} = r^{-6}$ and $\chi_{\rm M} = \exp[-\mathcal{A}(r-1)]$. In terms of specific parameters, $D = -A^2/4B$ and $R_e = (2B/A)^{1/6}$ for the Lennard Jones case while $\mathcal{A} = aR_e$ ($\mathcal{A} = 2.5$ for results exhibited here) for the Morse potential. In terms of $\chi(r)$, the partition function for both $V_{\rm LJ}$ and $V_{\rm M}$ is $Z = R_e \exp\varepsilon \int_0^\infty \exp[\chi(r)-1]^2 \exp[-\eta r] dr$.

Although one could in principle expand $\chi(r) - 1$ about $r = 1$, where the potential basin is locally parabolic, the significant departure from harmonic character with the shift from the condensed phase ($r \approx 1$) to the gaslike phase ($r \gg 1$) hampers a perturbative analysis of this kind. For a treatment which offers good convergence with only a handful of terms, and which provides a good description of the condensed and dissociated states alike, we consider the substitution $u = \chi(r)$, obtaining

$$Z = -R_e e^{\varepsilon} \int_0^\infty e^{-\varepsilon(u-1)^2} e^{-\eta \chi^{-1}(u)} \frac{1}{\frac{d}{du}\chi^{-1}(u)} du \qquad (1)$$

Integrating by parts, neglecting boundary terms, and using $v = u - 1$ leads to

$$Z = \frac{2R_e\varepsilon}{\eta} e^{\varepsilon} \int_{-1}^\infty e^{-\varepsilon v^2} e^{-\eta\chi^{-1}(v+1)} v dv \qquad (2)$$

which may be evaluated as a series of Gaussian integrals by Taylor expanding $\exp[-\eta\chi^{-1}(v+1)]$ about $v = 0$ with

$$e^{-\eta\chi^{-1}(v+1)} = e^{-\eta}\left[1 - \eta d_1 v + \frac{1}{2!}(\eta^2 d_1^2 - \eta d_2)v^2 + \ldots\right] \qquad (3)$$

where the d_i are ith derivatives of $\chi^{-1}(v+1)$ evaluated at $v = 0$. For $V_{\rm LJ}$, $d_1 = -1/6$, $d_2 = 7/36$, and $d_3 = -91/216$ while for $V_{\rm M}$, $d_1 = -1/\mathcal{A}$, $d_2 = 1/\mathcal{A}$, and $d_3 = -2/\mathcal{A}$.

For the sake of a quantitatively accurate description of the dissociation transition, it is important not to neglect the finiteness of the lower integration limit in evaluating the Gaussian integrals, which must be taken into consideration to account for dissociation. In the regime of interest, Z is well represented by

$$Z = e^{\varepsilon-\eta}\Big[e^{-\varepsilon}(\eta^{-1} + d_1) - \frac{\sqrt{\pi}}{4}\varepsilon^{-3/2}(4\varepsilon d_1 + d_1^3\eta^2 - 3\eta d_1 d_2 + d_3)\Big] \qquad (4)$$

where we have used $\int_{-1}^\infty \exp(-\varepsilon v^2) v dv = \exp -\varepsilon/(2\varepsilon)$, $\int_{-1}^\infty \exp(-\varepsilon v^2) v^2 dv \approx (\sqrt{\pi}/2)\varepsilon^{-3/2} - \exp -\varepsilon/(2\varepsilon)$ (i.e. retaining the leading term in the asymptotic series); we have neglected $\int_{-1}^\infty \exp(-\varepsilon v^2) v^3 dv$, and truncated $\int_{-1}^\infty \exp(-\varepsilon v^2) v^4 dv$ at $(3\sqrt{\pi}/4)\varepsilon^{-5/2}$.

For a description valid for both the condensed and gaslike phases, we obtain from Z rational expressions for observables of interest where typically leading and next to leading order terms in η and ε are retained in the numerator and the denominator; we calculate and discuss in turn the thermally averaged bond length $\langle l\rangle$, the internal energy $\langle E\rangle$, the specific heat c_p, and the thermal expansion coefficient α.

With the mean interatomic separation being $-R_e \partial \ln Z/\partial\eta$, the normalized thermally averaged bond length is well approximated with

$$\frac{\langle l\rangle}{R_e} = 1 + \eta^{-1}\left[\frac{e^{-\varepsilon} - \frac{3}{4}\sqrt{\pi} d_1 d_2 \varepsilon^{-3/2}\eta^2}{e^{-\varepsilon} - \frac{\sqrt{\pi}}{4}\varepsilon^{-3/2}\eta\,(4d_1\varepsilon + d_3)}\right] \qquad (5)$$

readily inverted via the quadratic formula to obtain η in terms of $\langle l\rangle$. Asymptotically, for $\eta \ll \varepsilon$, the residual component of the mean separation (small in the condensed phase but diverging with the dissociation transition) may be represented by the simpler expression $\tilde{\Delta}_l \equiv (\langle l\rangle/R_e - 1) = \varepsilon^{1/2}\exp -\varepsilon/(d_1\sqrt{\pi}\eta^2)$.

To more conveniently visualize $\langle l\rangle$, (as well as $\langle E\rangle$, α, and c_p), we choose ε for the abscissa where only T is varied while holding p fixed for a given curve; $\varepsilon \gg 1$ and $\varepsilon \ll 1$ correspond to the low and high T regimes respectively. Whereas $\gamma = pR_e/D$ remains constant, $\eta = \beta p R_e = \gamma\varepsilon$ varies with temperature.

Figure 1 displays results corresponding to $V_{\rm LJ}$ in panel (a) and $V_{\rm M}$ in panel (b) with open symbols indicating numerical results and solid curves representing the foregoing approximations to $\langle l\rangle$. The black traces, calculated with the rational expression in Eq. 5, are in good quantitative agreement with numerical data even for $\gamma = 1.0$. On the other hand, the $\tilde{\Delta}_l + 1$ approximation is represented by lighter (red/blue for $V_{\rm LJ}/V_{\rm M}$) curves, and accurately indicates the location where $\langle l\rangle$ begins to diverge significantly from R_e. Moreover, despite the simple structure, good agreement with exact numerical results is evident for $\gamma < 0.01$.

To estimate γ for physically realistic systems, we consider a chain of noble gas atoms (e.g. Argon) in the context of the Lennard Jones Model or a covalently bonded pair of atoms (e.g. H_2) in the Morse potential framework in a 1D conduit. With typical atomic radii on the order of an Ångstrom, we assume a cross sectional area on the order of $(1\ \text{Å})^2 = 10^{-20}\ \text{m}^2$. Using 1.01×10^5 Pa for standard atmospheric pressure, find $p \sim 10^{-15}$ J/m. In the case of Argon, one has $D = 0.011$ eV and $R_e = 3.8$ Å [5–8] and $\gamma = 2.2\times10^{-4}$. On the other hand, for H_2, $D = 4.52$ eV [9] and we take R_e to be the measured bond length of 0.74 Å [10]; one obtains $\gamma = 1.0\times10^{-7}$, with both γ values deep in the $\gamma \ll 1$ range.

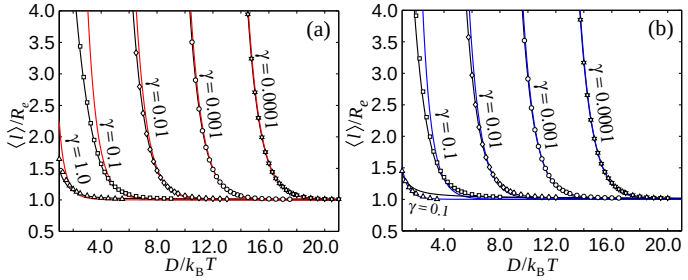

FIG. 1: (Color online) Normalized mean atomic separations for the Lennard Jones (left panel) and Morse potential (right panel) for various γ values; solid traces are analytical approximations while open symbols are numerical data. Black curves correspond to the $\tilde{\Delta}_l + 1$ relationship, while colored traces represent the rational $\langle l\rangle$ expression.

The internal energy, $\langle E\rangle$, is well approximated as

$$\frac{\langle E\rangle}{k_BT} = \eta - \varepsilon + \frac{e^{-\varepsilon}\eta^{-1}(1+\varepsilon) - \varepsilon^{-3/2}\frac{\sqrt{\pi}}{8}(4d_1\varepsilon + 3d_3)}{e^{-\varepsilon}\eta^{-1} - \varepsilon^{-3/2}\frac{\sqrt{\pi}}{4}(4d_1\varepsilon + d_3)} \tag{6}$$

To strip away trivial dependencies, Figure 2 shows the residual internal energies, $E_{\rm Res} = \langle E\rangle + D - pR_e$, with Lennard Jones results in the main panel and Morse potential results in the inset for a variety of γ values. Solid curves obtained from the rational expression closely coincide with the open symbols representing numerical data. Though $E_{\rm Res}$ tends to $k_BT/2$ for sufficiently large ε, the expected dependence where $\langle l\rangle \approx R_e$ where anharmonicities are negligible, the residual energy component is non-monotonic. One sees from the main graph and the inset graph that the breadth and height of the peak separating the low and high T regimes scales asymptotically as $\log_{10}(1/\gamma)$

The specific heat at constant pressure is $c_p = \partial\langle E\rangle/\partial T$, which is

$$\frac{c_p}{k_B} = \frac{\frac{1}{2}\varepsilon^2\left(\varepsilon + \frac{3d_3}{2d_1}\right) - \Upsilon\varepsilon^{1/2}\left(1 + \varepsilon + \frac{d3}{4d_1}\right) + \Upsilon^2}{\varepsilon^{-2}\left(\varepsilon + \frac{d_3}{2d_1}\right) - 2\Upsilon\varepsilon^{-3/2}\left(\varepsilon + \frac{d3}{4d_1}\right) + \Upsilon^2} \tag{7}$$

where $\Upsilon = \exp -\varepsilon/(\sqrt{\pi}\eta d_1)$.

Specific heat results are displayed in the main graph (for $V_{\rm LJ}$) and the inset (for $V_{\rm M}$) of Fig. 3 for a range of γ values; as in the case of the internal energy, there is good agreement among the analytical (solid curve) and the numerical (open symbols) results.

One sees from the analytical c_p expression in Eq. 7 and the curves in Fig. 3 that the specific heat tends to k_B for sufficiently low D (i.e. higher T) and flattens to $k_B/2$ for $D \gg 1$ (low T). Whereas the latter is a hallmark of the condensed phase, the former is expected for a dissociated system; the transition between the two asymptotically flat regions is non-monotonic, with a peak separating the k_B and $k_B/2$ regimes. The region where c_p rises to a

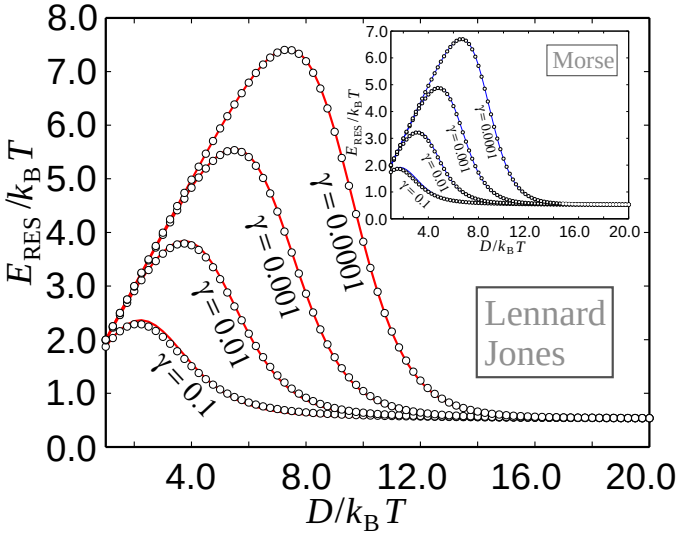

FIG. 2: (Color online) Residual internal energy results for various γ values with the main graph showing Lennard Jones results and the inset displaying Morse results. Solid traces represent analytical results, while open symbols indicate numerical data.

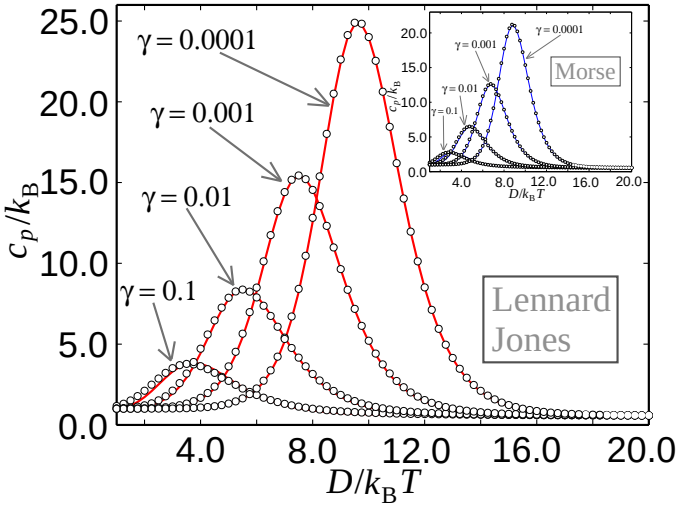

FIG. 3: (Color online) Specific heat curves for assorted γ values with Lennard Jones results in the main graph and Morse results in the inset. Analytical results are shown as solid traces, while open symbols represent numerical data.

peak, representing the dissociation transition, becomes taller and narrower with decreasing γ.

The coefficient of thermal expansion $\alpha = \langle l\rangle^{-1}\partial\langle l\rangle/\partial T$ is well represented by

$$\frac{\alpha}{k_B} = \frac{\frac{3}{4}\eta d_2\varepsilon^{-1} - \Upsilon\varepsilon^{1/2}\left(\varepsilon + \frac{3}{2} + \frac{d_3}{4d_1} - \frac{3\eta d_2}{2}\right) + \Upsilon^2}{\eta - \Upsilon\varepsilon^{-1/2}\left(\varepsilon + 2\eta\varepsilon + \frac{d_3}{4d_1}\right) + \Upsilon^2} \tag{8}$$

Juxtaposed analytical (solid traces) and numerical results (open symbols) are shown in Figure 4 for various

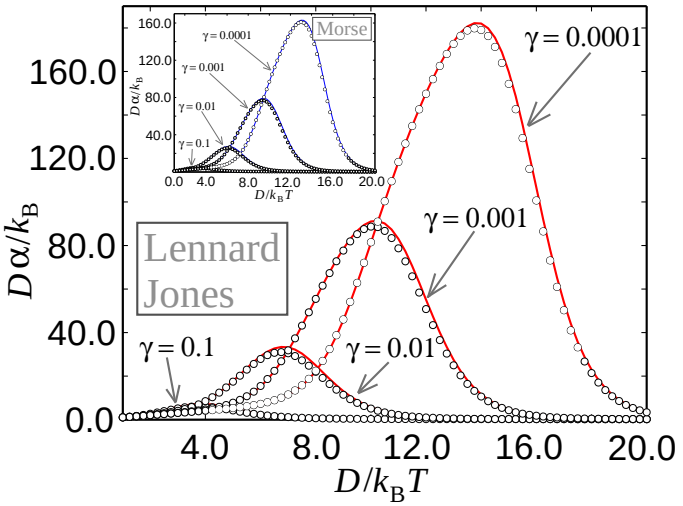

FIG. 4: (Color online) Thermal expansion coefficient results for a range of γ values with Lennard Jones results plotted in the main graph and corresponding results for the Morse potential in the inset. Solid curves represent analytical results, while open symbols indicate numerical data.

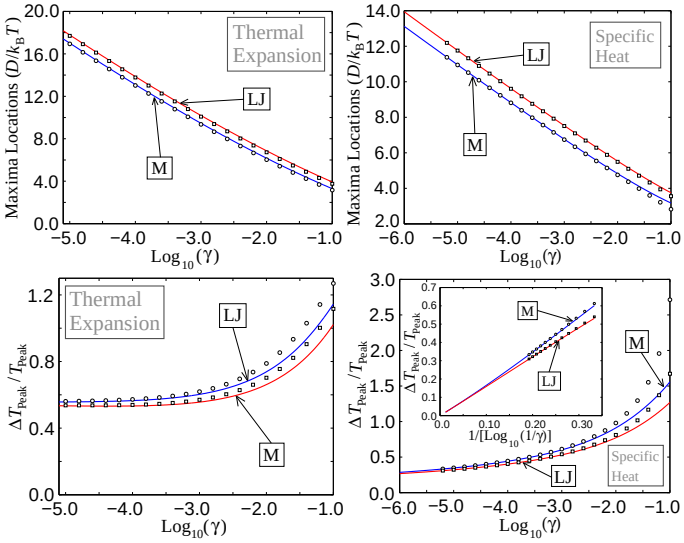

FIG. 5: (Color online) Peak locations for the specific heat (upper right panel) and thermal expansion coefficient (upper left panel). Corresponding relative full width half maxima (i.e. $\Delta T_{\rm peak}/T_{\rm peak}$) appear in the lower right and lower left panels for the specific heat and coefficient of thermal expansion respectively. Throughout, open squares represent Lennard Jones results and open circles Morse results.

γ values with $D\alpha/k_{\rm B}$ on the vertical axis. As in the case of the specific heat, the α curves are non-monotonic, with peak heights increasing with decreasing γ. Choosing $D\alpha/k_{\rm B}$ for the ordinate is in part to show the slow convergence to the low T value of $3d_2/4$ in the $\gamma \ll 1$ limit. All of the cases shown correspond to experimentally realistic γ values, and in all but one of the curves shown, α is appreciably different from the limiting value even for ε as high as 10.

The peak locations calculated in the framework of the analytical approximations (solid traces) for c_p and α are in close agreement with the exact numerical results (open symbols) as may be seen in the upper panels of Fig. 5. In statistical mechanics singularities are not in general encountered for single component systems, with non-analytic behavior emerging only in thermodynamic limit as the number of degrees of freedom tends to infinity. Nevertheless, the low pressure regime is atypical in the sense that singular behavior is inevitable as p (or γ) tends to zero due to the divergence of $\langle l\rangle$ for any finite T as $p \to 0$. Hence, the possibility of a sharp dissociation transition for $\gamma \ll 1$ must be examined with care.

As a measure of the extent to which the dissociation transition is singular, the sharpness of the thermal expansion coefficient and specific heat peaks is quantified in the lower panels of Fig. 5 as the relative full width half maximum, $\Delta T_{\rm Peak}/T_{\rm Peak}$. In the case of α, $\Delta T_{\rm Peak}/T_{\rm Peak}$ tends to a finite value common to both $V_{\rm LJ}$ and $V_{\rm M}$, indicating the α peaks cease to become narrower relative to their location with decreasing γ.

On the other hand, the specific heat relative peak width appears to tend to zero with decreasing γ, a trend highlighted in the lower right panel inset of Fig.5 showing $\Delta T_{\rm Peak}/T_{\rm Peak}$ relative to $1/\log_{10}(\gamma^{-1})$, The curves are asymptotically linear as $\gamma \to 0$, with the relative peak width vanishing for $p \to 0$ as singular behavior appears.

In conclusion, with a nonperturbative treatment of the anharmonicity of interatomic potentials, we provide a theoretical description of the dissociation transition valid for the condensed state as well as the gas-like phase where thermal fluctuations have driven pairs of atoms far from their equilibrium separations. By applying a unified treatment to disparate potentials, we have obtained analytical results for salient thermodynamic observables in good agreement with precise numerical results. Though ascribed to distinct bonding physics, there are striking similarities in results, e.g. with $\langle l\rangle/R_e = 1 + \varepsilon^{1/2}\exp -\varepsilon/(d_1\sqrt{\pi}\eta^2)$ specifying the mean bond length for $\gamma \ll 1$.

Useful conversations with Michael Crescimanno are gratefully acknowledged.

[1] J. E. Lennard-Jones, Proc. R. Soc. Lond. A **106** (738), 463 (1924).
[2] P .M. Morse, Phys. Rev. **34**, 57 (1929).
[3] J. S. Dugdale and D. C. K. MacDonald, Phys. Rev. **96**, 57 (1954).
[4] J. S. Dugdale and S. K. Roy, Phys. Rev. **97**, 673 (1955).
[5] A. Rahman, Phys. Rev. 136, A405 (1964).
[6] J. A. Barker, R. A. Fisher, and R. O. Watts, Molecular Physics **21**, 657 (1971).

[7] L. A. Rowley, D. Nicholson, and N. G. Parsonage, Journal of Computational Physics **17**, 401 (1975).
[8] John A. White, J. Chem. Phys. **111**, 9352 (1999).
[9] S. J. Blanksby and G. B. Ellison, Acc. Chem. Res. **36** (4), 255 (2003).
[10] H. B. Gray, *Chemical Bonds: An Introduction to Atomic and Molecular Structure*, (University Science Books, Sausalito, California, 1994).